6 June 2025

High-throughput Triazole-based Combinatorial Click Chemistry for the Synthesis and Identification of Functional Metal Complexes

David R. Husbands[1], Ça#r# Özsan[2,1], Athi Welsh[2,1], Richard J. Gammons[1], Angelo Frei[1,2]

1. University of York
2. University of Bern

Abstract

A new high-throughput combinatorial approach using CuAAc “Click” chemistry has been implemented to make 192 bidentate pyridyl-1,2,3-triazole ligands. This ligand library was coordinated to five metal scaffolds under mild conditions to yield 672 novel metal compounds, representing a novel methodology for the accelerated exploration of the transition metal complex chemical space. The prepared libraries have been showcased for compound discovery primarily in antimicrobial applications, with selected libraries further tested for catalytic and photophysical screening. We demonstrate the versatility of combinatorial metal complex synthesis by screening all crude mixtures for antibacterial activity and cytotoxicity, enabling the rapid identification of hit compounds. Six promising metalloantibiotics have been identified and re-synthesized, exhibiting activity against Gram-positive bacteria in the nanomolar range with favorable therapeutic windows. The reported methodology represents a significant expansion in the field of metal-based combinatorial chemistry and its application towards the systematic coverage of vast chemical spaces in the search for novel molecules with optimized properties.

Keywords

High-throughput, Combinatorial Chemistry, Metalloantibiotics, Click Chemistry, Ruthenium, Iridium, Manganese, Rhenium, Catalysis

High-throughput Triazole-based Combinatorial Click Chemistry for the Synthesis and Identification of Functional Metal Complexes

*David R. Husbands[1], Çağrı Özsan[1,2], Athi Welsh[1,2], Richard J. Gammons[1], Angelo Frei[1,2]**

[1] Department of Chemistry, University of York, York YO10 5DD, U.K.

[2] Department of Chemistry, Biochemistry & Pharmaceutical Sciences, University of Bern, Freiestrasse 3, 3012 Bern, Switzerland

Abstract

A new high-throughput combinatorial approach using CuAAc "Click" chemistry has been implemented to make 192 bidentate pyridyl-1,2,3-triazole ligands. This ligand library was coordinated to five metal scaffolds under mild conditions to yield 672 novel metal compounds, representing a novel methodology for the accelerated exploration of the transition metal complex chemical space. The prepared libraries have been showcased for compound discovery primarily in antimicrobial applications, with selected libraries further tested for catalytic and photophysical screening. We demonstrate the versatility of combinatorial metal complex synthesis by screening all crude mixtures for antibacterial activity and cytotoxicity, enabling the rapid identification of hit compounds. Six promising metalloantibiotics have been identified and re-synthesized, exhibiting activity against Gram-positive bacteria in the nanomolar range with favorable therapeutic windows. The reported methodology represents a significant expansion in the field of metal-based combinatorial chemistry and its application towards the systematic coverage of vast chemical spaces in the search for novel molecules with optimized properties.

Introduction

The Copper(I)-catalyzed Alkyne–Azide cycloaddition (CuAAc) "Click" reaction to form substituted 1,2,3-triazoles (hereafter referred to as "triazoles") is one of the cornerstones of modern chemistry.[1] High functional group tolerance, bio-compatible coupling conditions and high yields make it a powerful transformation. Although mostly used as a convenient way of linking molecular fragments together, it is possible for the resulting triazole unit to bind to metal centres as a ligand. This coordination opens up avenues for catalysis and complexes with highly tuneable photophysical properties.[2,3] Incorporation of a pyridine or other lone pair donating group to the triazole compound enables formation of bidentate ligands, which are able to chelate metal centres effectively *via* 5- and 6-membered metallocycles (Figure 1).[4] The binding modes of these ligands can be varied by switching the substitution site on the triazole ring (through different pyridine/azide structures), giving ligands with substantially different chemistries.[5] Coordination tends to occur through the more electron rich N3, giving more stable complexes, while coordination through the more electron deficient N2 is much rarer and can cause instability in complexes (Figure 1).[6] Triazoles can also coordinate to metals as *N*-heterocyclic carbenes rather than through the N donors.[7]

From our perspective, the coordination chemistry of these triazole ligands holds great promise for the development of new metal-based antibiotics.[8] This area is becoming increasingly relevant due to the rise of antimicrobial resistance (AMR) to the current arsenal of antibiotics, which has been designated by the WHO as one of the top global health threats.[9,10] Concurrently, there are very few new antibiotics being developed, with only 19 new antibacterial drugs being approved for use between 2013 – 2023, and of these only 2 represent a new chemical class.[11]

There have been several examples of bidentate pyridyl-triazole ligands being used for therapeutic applications, from using CuAAc-formed triazoles to anchor sulfonamide drugs to metal centres (increasing activity against methicillin-resistant *Staphylococcus aureus* (MRSA), Figure **1A**),[12] to using bidentate triazole ligands directly in forming tris-homoleptic ruthenium $[Ru(L)_3]^{2+}$ complexes (showing broad spectrum antibiotic properties, Figure **1B**)[13], tris-homoleptic osmium *mer*-$[Os(L)_3]^{2+}$ complexes (photoactive against MRSA, Figure **1C**)[14] and rhenium(I) carbonyl complexes (displaying activity *vs*. both Gram-positive and Gram-negative bacteria).[15] Additionally, similar bidentate pyridyl-triazoles have

been coordinated to a manganese(I) tricarbonyl scaffold, utilising Clotrimazole as an axial ligand, and were demonstrated to be active against Gram-negative bacteria (Figure **1D**).[16] In terms of other therapeutical applications, a ruthenium(II) arene (Figure **1E**) scaffold was coordinated to derivatized sugar pyridyl-triazole ligands (selective activity against ovarian cancer cells)[17], and pyridyl-triazole ligands were used to coordinate cyclometallated iridium(III) scaffolds, generating several compounds with photoluminescence properties (Figure **1F**).[18] These could be relevant for photodynamic therapy applications against either bacteria or cancer cells, similar to recent work on similar cyclometallated complexes by Kench *et al.*[19,20] Platinum compounds containing triazole ligands or linkers have also been investigated for cancer therapies.[21] Although an impressive array of compounds has been made utilising triazole ligands, it should be noted is that in almost all cases, only a handful of individual complexes have been synthesized and tested for their intended applications. One of the reasons for this is the synthesis of the triazole ligand, which requires an azide to be generated as a precursor. Azide formation typically occurs in batch *via* a reaction between NaN_3 and an aryl/alkyl bromide, requiring forcing conditions and undesirable solvents, and can generate significant impurities.[22,23]

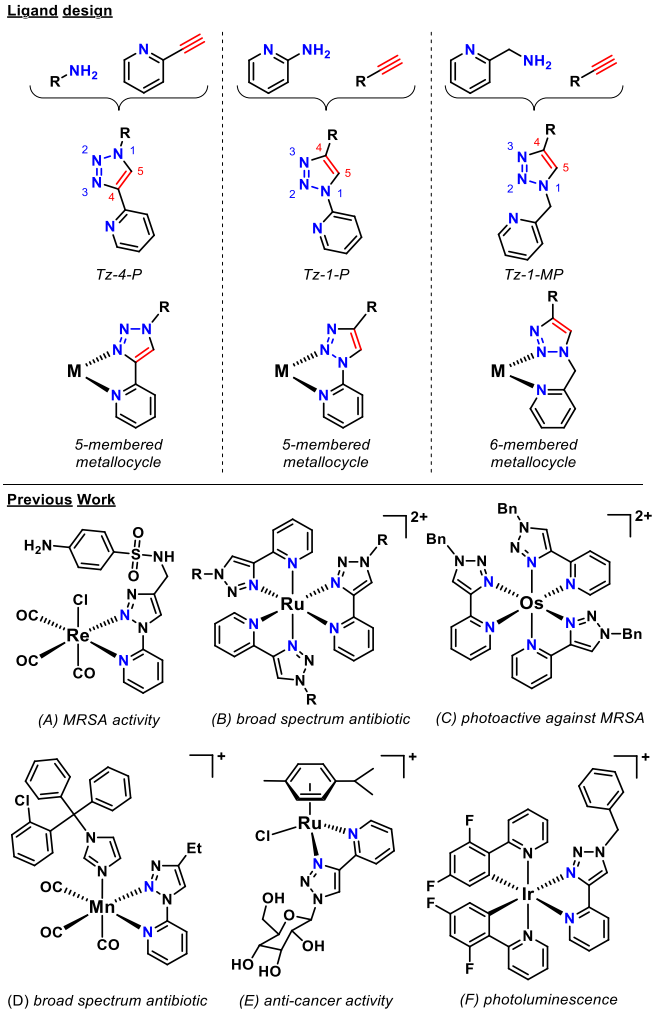

Figure 1: (Top) pyridyl-triazole ligand potential building blocks, numbering convention used in this paper and coordination modes to metal centres.[5] (Bottom) Previous Work – examples of pyridyl-triazole metal complexes for a range of applications; (**A**) Re-based sulfonamide anchored complex;[12] (**B**) tris(homoleptic) Ru complexes;[13] (**C**) tis(homoleptic) *mer*-Os complex;[14] (**D**) $Mn(CO)_3$-Clotrimazole complex;[16] (**E**) RuCy complex with a coordinated sugar derivative;[17] (**F**) cyclometallated IrCN complex.[18]

New developments by Meng *et al.*[24] have opened the door to high-throughput synthesis of this class of ligands through sulfur(VI) fluoride exchange (SuFEx) chemistry under ambient conditions, efficiently generating azides *in situ* from virtually any primary amine. We envisaged that this methodology could be used to generate substantial and varied libraries of pyridyl-triazole based ligands. Coordination of this library to various metal scaffolds in a similar vein to previous work by our group and others using

combinatorial chemistry approaches with Schiff-base ligands[25–27] would allow us to create libraries of novel complexes. These would in turn be screened for antibacterial hits, toxicity towards mammalian cells and other potential areas of discovery such as catalysis and photophysical applications. It should be noted that these ligands offer stability benefits over Schiff-base type counterparts, which are prone to hydrolysis and degradation in the presence of acid or base.

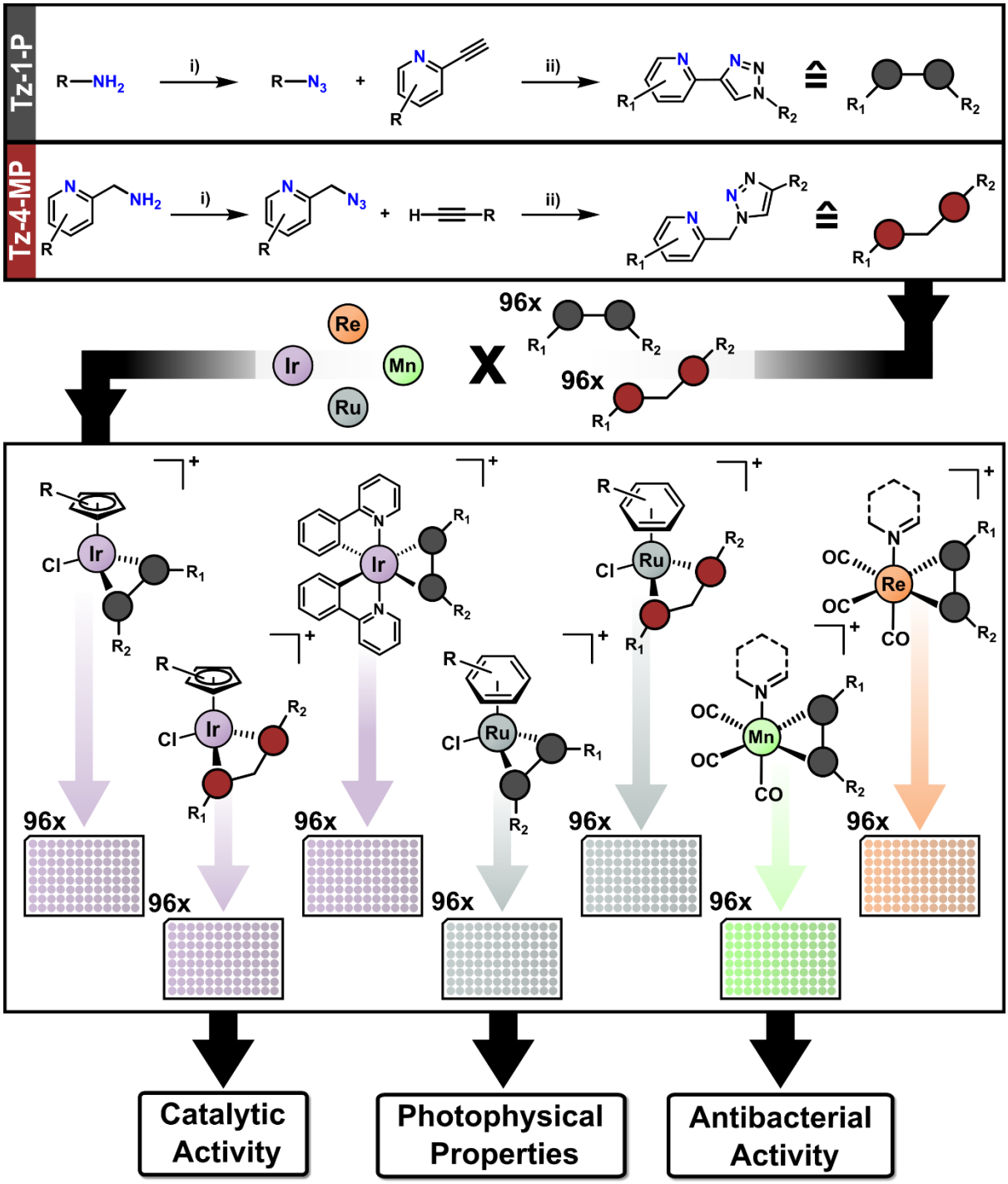

Figure 2: Overview of the combinatorial methodology presented in this work. Conditions for i) Amine (80 mM) FSO_2N_3 (1.05 equiv.), $KHCO_3$ (4 equiv.), MTBE/DMSO/H_2O (11:84:5), r.t., 18 h; conditions for ii) Alkyne (80 mM, 1 equiv.), sodium ascorbate (0.5 equiv), $CuSO_4$ (2.5 mol%), $(BimH)_3$ (2.5 mol%), DMSO/H_2O (3:1), r.t., 18 h; to give the triazole library at 20 mM concentration (for more details, see SI Section 2.1). Details of the coordination of the triazole libraries with metal can be found in Figure 3.

Results and Discussion

Ligand Library Creation

We began by optimising the conditions described by Meng *et al.*[24] for the *in situ* generation of azides from primary amines, followed by CuAAc Click reactions with 2-alkynepyridines. Initially, significant alcohol impurities were observed, but this was remedied by changing the copper ligand from tris-hydroxypropyltriazolylmethylamine (THPTA) to tris(2-benzimidazolylmethyl)amine ($BimH)_3$. Additionally, we found that the reported phosphate buffer was not required in our system, and low catalyst/ligand loadings of 2.5 mol% were sufficient. With the optimized conditions in hand, we used an Opentrons liquid handling robot to generate a library of 96 triazole-4-pyridine (**Tz-4-P**) compounds (24x amines, 4x 2-alkynepyridines, Figure **3A**). The success of these couplings was verified by LC-MS (Figure 4). A further library of 96 triazole-1-methylpyridine (**Tz-1-MP**) compounds (12x alkynes, 8x 2-picolylamines, Figure **3B**) was prepared using the same method. Under the same conditions, we also attempted to couple 2-aminopyridine with alkynes to generate a Tz-1-P library, but this was unsuccessful.

The average conversion efficiency (as determined by automated LC-MS chromatogram integration at 254 nm)[28] was 75 ± 16%, showing that despite the structural diversity of the amines a generally high conversion efficiency was observed (Figure 4). In terms of trends across the formation of this library, the electron withdrawing ester group on **M11** tended to lead to lower conversions (both for the initial click reaction, and for subsequent coordination), although other electron deficient amines (**M13**, **M17**) seem to form ligands in high yielding reactions comparable to electron rich systems (**M12**, **M19**). As such, it does not appear that the electronics of the amine building blocks have a significant effect on the outcome of the initial CuAAc reaction. The LC-MS traces of ligands containing 7-aminocephalosporanic acid and ampicillin (**M15**, **M16** respectively) were not as clean as the others, and it was found that these ligands and their metal compounds slowly degrade over time in solution (See Supporting Information (SI) Figures S10-11). However, it was decided to include them in further testing as they represented more complex structures with β-lactam motifs, and ideally the coordination of these derivatives to metal centres would enhance their biological effects.[29] On a practical level, it was discovered that several of the target ligands were poorly soluble in DMSO, so tended to precipitate or crystallize out of solution. This was especially prevalent among **Y4** ligands, where the pyridyl bromine group seems to have significantly affected solubility. This was remedied by pulverising the affected samples through sonication and aspirating the mixture to homogenize it before dispensing the ligands for further reactions.

Similarly, the **Tz-1-MP** library was synthesized with a high average conversion efficiency (77 ± 12 %), with no noticeable degradation of the products (Figure 5). Initial tests included two aliphatic alkynes (cyclohexylacetylene and cyclopropylacetylene), but the products of these reactions were not observable by LC-MS. As these alkynes also exhibited problematic volatility, it was decided that only aromatic alkynes would be used. These were in turn limited to relatively simple derivatives, which does demonstrate a limitation of using aromatic alkynes (**Tz-1-MP**) compared to primary amines (**Tz-4-P**) for the triazole formation. Conversely, the use of picoline-derived amines allowed for a substantially larger variety in the pyridine fragment of the ligand compared to the **Tz-4-P** library, with several halogenated derivatives included. Although the overall structural variety of the **Tz-1-MP** library is not as broad as **Tz-4-P**, the overall conversion is comparable, with only **A3** (highly electron-deficient *p*-nitro group) and **P4** showing consistently lower conversions. There were no solubility issues observed with the **Tz-1-MP** library.

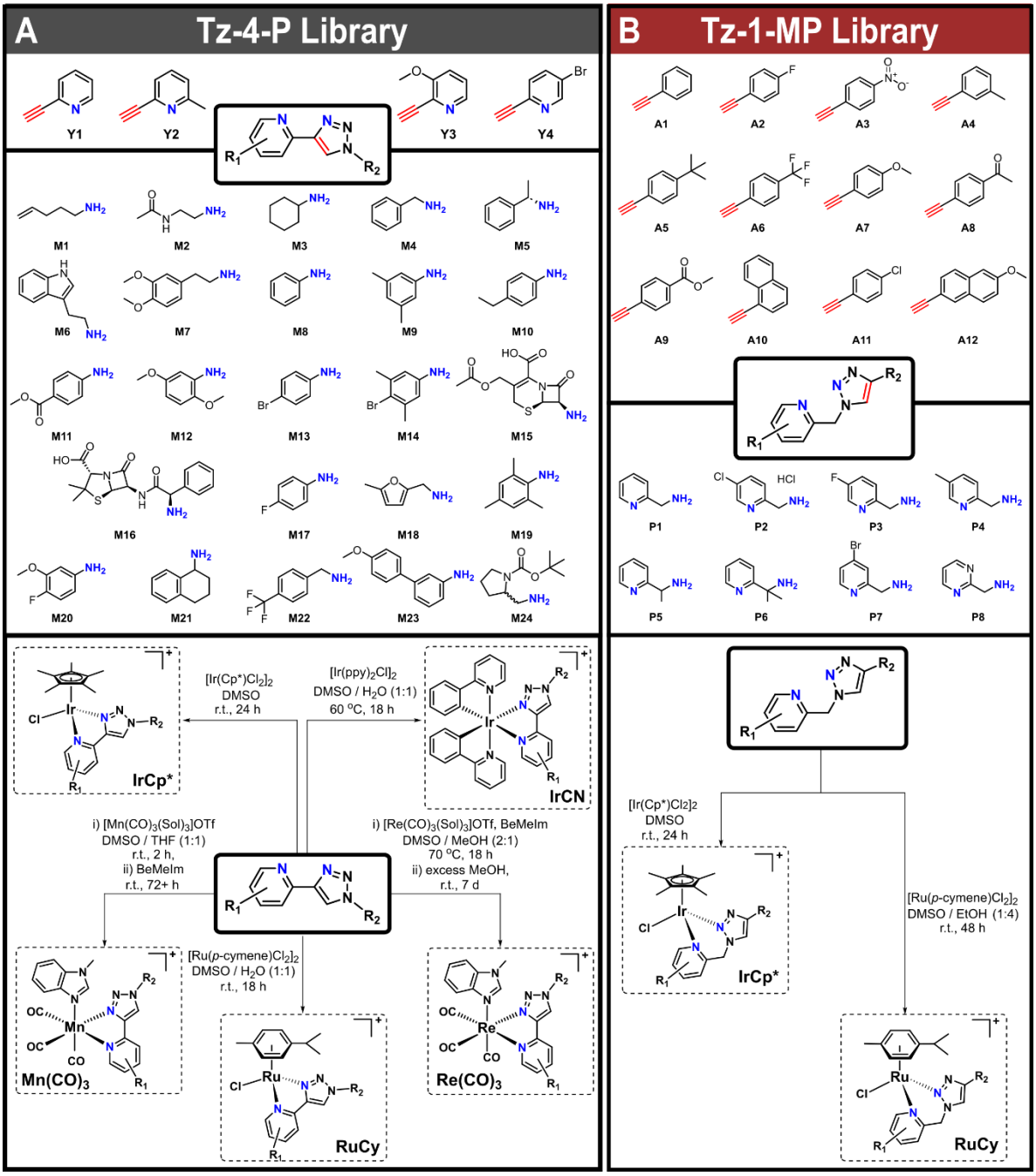

Figure 3: Overview of amine and alkyne building blocks utilized for the **Tz-4-P** (**A**) and **Tz-1-MP** (**B**) libraries and synthetic schemes and conditions for the coordination of the **Tz-4-P** and **Tz-1-MP** libraries to metal scaffolds to form the metal complex libraries.

Metal Library Synthesis and Characterisation

After test coordination reactions using **M4Y1** to optimize conditions, the entire **Tz-4-P** library was coordinated to the following metal scaffolds (Figure **3A**): $[Ir(ppy)_2Cl]_2$ (ppy = 2-phenylpyridine, **IrCN**), $[IrCp^*Cl_2]_2$ (**IrCp***), $[Ru(p\text{-cymene})Cl_2]_2$ (**RuCy**), $Re(CO)_5Cl$ (**Re(CO)$_3$**) and $Mn(CO)_5Br$ (**Mn(CO)$_3$**). Both manganese and rhenium scaffolds were pre-activated with silver triflate, and solvent libraries without 1-benzyl-2-methylimidazole (BeMeIm) as an axial ligand were also generated as controls. The reaction mixtures for the five different metal complex libraries were setup simultaneously in a high-throughput manner using the Opentrons OT2 liquid handling robot.

Coordination of the **Tz-4-P** library to the **IrCN** scaffold was achieved under conditions far less forcing than current literature procedures, which require toxic, high boiling point solvents, temperatures >150 °C, or microwave conditions.[19,30] In our procedure, high conversion was achieved by heating the ligands and $[Ir(ppy)_2Cl]_2$ dimer in a 1:1 mixture of DMSO:H_2O at 60 °C for 18 h. **IrCp*** and **RuCy** libraries were generated in good purity under ambient conditions. The **IrCp*** library is being explored in an ongoing project, so will not be discussed further here.

For the **Re(CO)$_3$** library, poor conversion to the target complexes was initially obtained (1:2 MeOH: DMSO, 70 °C, 18 h). After addition of an excess of MeOH, the reaction crudes were left standing for one week at room temperature to allow for the solvent to evaporate, giving significantly improved product yields. This is likely due to DMSO solvent competitively binding with the rhenium scaffold instead of BeMeIm. A similar effect was observed for the **Mn(CO)$_3$** library, as when conversion is low, the byproduct is often the solvent adduct (*e.g.* **Mn(CO)$_3$M2Y3**, see SI Figures S12-13). Previously, our group has shown that manganese (I) carbonyl complexes with solvent as the axial ligand tend to have low antibacterial activity.[27] It should also be noted that manganese(I) tricarbonyl complexes are often light-sensitive, hence this library was prepared, handled, tested and stored in the dark.

Test coordination to the same scaffolds using **Tz-1-MP** (**P1A1**) implied that DMSO bound competitively with all metal centres, preventing coordination in many situations, even at elevated temperatures. The exception to this was the $[IrCp^*Cl_2]_2$ scaffold, which yielded product and led to the creation of an **IrCp*** library (Figure **3B**). In addition, excess EtOH with $[Ru(p\text{-cymene})Cl_2]_2$ gave the desired complexation with **P1A1** in high yields, so complexation with the **Tz-1-MP** library was done in this case (**RuCy**, Figure **3B**).

The poor complexation of the **Tz-1-MP** library could be due to the greater flexibility imparted by the methyl linker, forming 6-membered metallocycles rather than 5-membered metallocycles formed by the more rigid **Tz-4-P** library. Generally, rigid 5-membered rings are significantly more stable than 6-membered rings due to fewer degrees of freedom and a more optimum “bite angle” (the angle between the donor groups and the metal centre).[31] More specific examples involving **Tz-1-MP** scaffolds from Urankar *et al*. show that under certain coordination conditions, these ligands can bind in a monodentate fashion through the triazole ring (to palladium) rather than a chelating effect.[32] Maisonial *et al.* similarly demonstrated that for triazoles with a pendant primary amine, 5-membered chelates were significantly more stable when coordinated to platinum than 6-membered metallocycles.[33]

For all libraries, the purity and identity of all compounds were assessed by LC-MS (all processed LC-MS spectra, target complex percentage conversion and retention time are supplied in the Supporting Information). Typically for metal-based combinatorial synthesis, libraries are only partially characterized (either random representative samples or predetermined subsets, *e.g.* using ^{19}F NMR for fluorine containing compounds) to reduce the time-consuming characterisation step to a more practical level.[25,30,34] In our case, the charged nature of the metal complexes makes them amenable to characterisation by LC-MS, a technique that itself can be highly automated both in collection and assessment of the data (see SI Section 2.9).

For **Mn(CO)$_3$**, and to a lesser extent the **Re(CO)$_3$** library, **Y2** containing ligands were consistently poor at coordination. This could be due to steric clashing of the pyridine methyl group with the axial ligands during coordination. Similarly, **Y4** containing ligands were performed poorly, possibly due to the lower solubility of the ligands, or electron withdrawing effect of the pyridyl *para*-bromine.

Generally, ligands formed from simple aryl amines such as **M8**, **M10** and **M17** tended to coordinate most efficiently. Our data also indicates that **M** group sterics do not affect the yields, likely due to these groups being spatially removed from the metal centre. Electronic effects seem to be more consequential, with strong electron donating units such as methoxy- and methyl-groups favoured. Aliphatic groups from building blocks such as **M1**, **M2** and **M3** also coordinated well, again implying the prevalence of electronic effects on coordination over steric influences.

For the **Tz-1-MP** library, coordination of the **P6** variants was consistently poor, likely due to the *gem*-dimethyl groups on the methyl linker. As well as being a useful functionality in medicinal chemistry,[35] it was envisaged that the Thorpe-Ingold effect would be beneficial to coordination, both increasing

rotational barriers and decreasing the bite angle of the ligand.[36] Instead, it appears that the steric bulk of the *gem*-dimethyl groups effectively inhibits chelation in **P6** containing ligands. In most other cases, coordination of this library to the metal centres was reasonably successful, and the general high yielding formation of this ligand library by CuAAc reaction is a testament to the robustness of the optimized Click conditions.

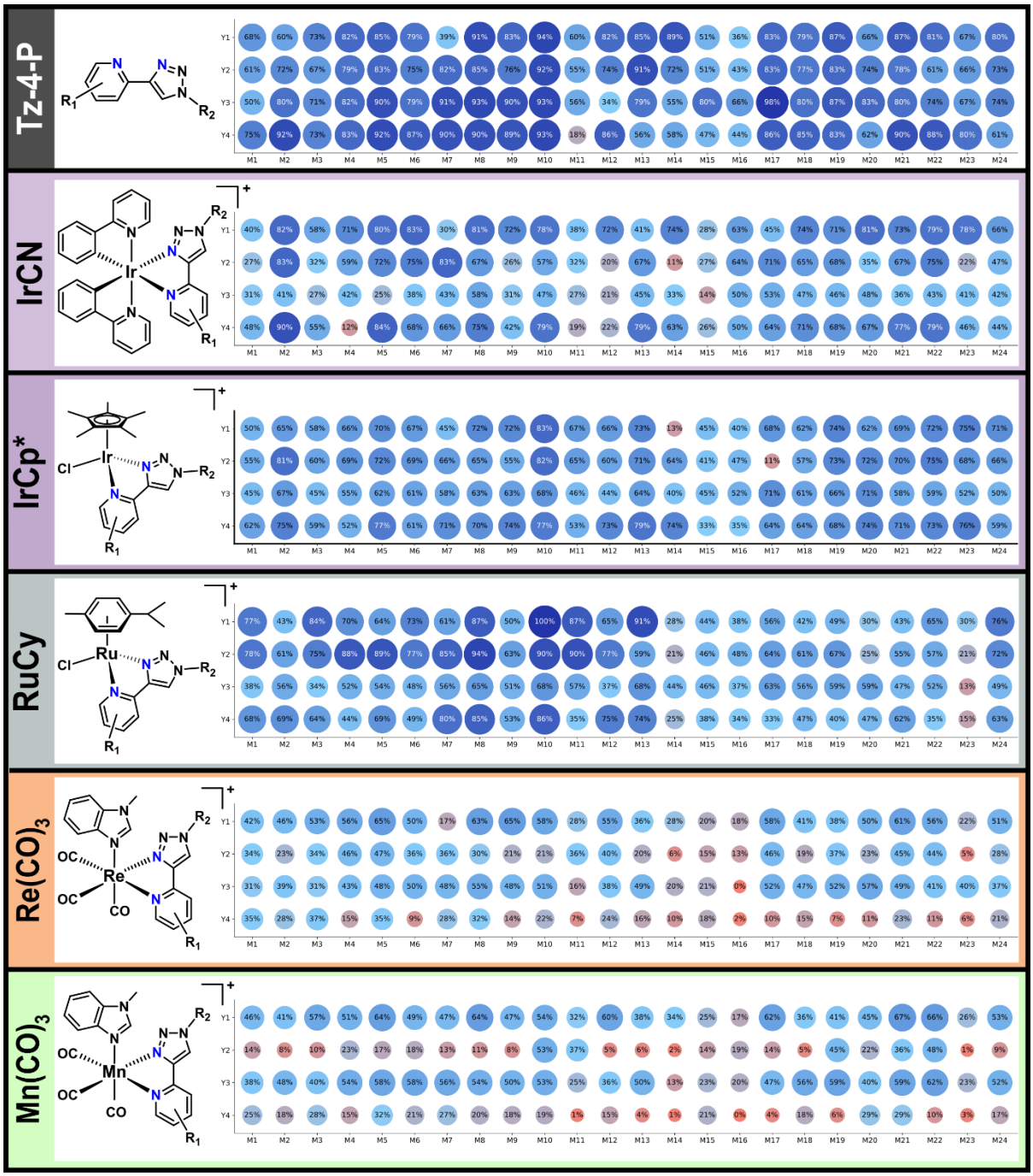

Figure 4: Purity of the **Tz-4-P** ligand and metal complex libraries, as ascertained by peak area% of the total from LC-MS data (254 nm). Compound peaks were identified automatically using the mass of the target ion and the corresponding UV peak was automatically integrated by custom Python scripts (SI Section 2.9). RuCy library conversions were normalized to 100% due to low UV response at 254 nm, and the conversions of IrCp* libraries is an aggregate of the parent ion (M^+) and the MeCN adduct (M^{2+}) peaks.

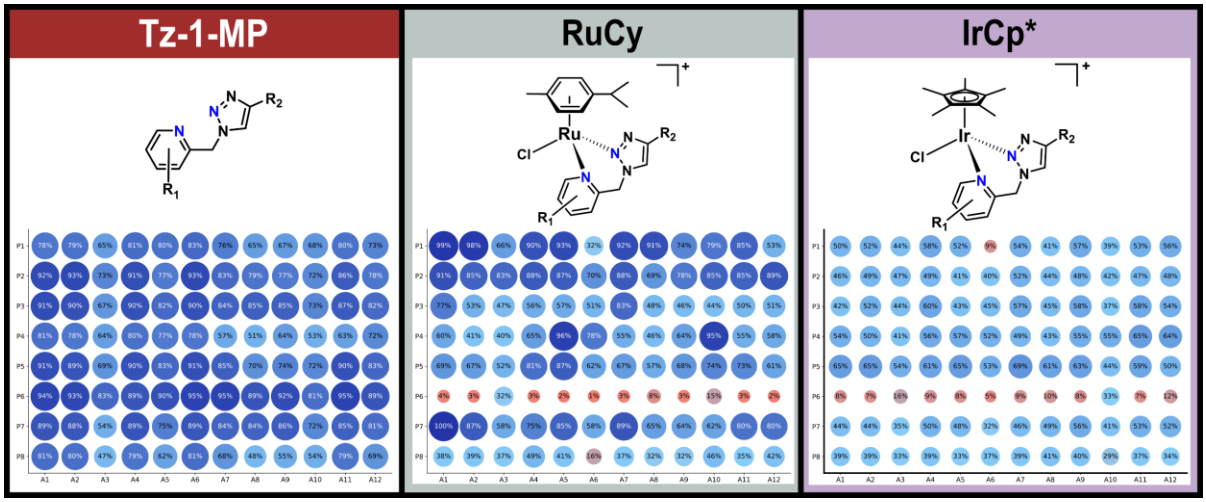

Figure 5: Purity of the **Tz-1-MP** ligand and metal complex libraries, as ascertained by peak area% of the total from LC-MS data (254 nm). Compound peaks were identified automatically using the mass of the target ion and the corresponding UV peak was automatically integrated by custom Python scripts (SI Section 2.9). RuCy library conversions were normalized to 100% due to low UV response at 254 nm, and the conversions of IrCp* library is an aggregate of the parent ion (M^+) and the MeCN adduct (M^{2+}) peaks.

Photophysical Properties

Taking inspiration from the work by Kench *et al.*, we investigated the photophysical properties of the **IrCN** library with the aim of exploring the possibility of photodynamic therapy.[19]. As can be seen in Figure 6, a range of fluorescence intensities were observed, but the maximum emission wavelength (λ_{max}) was evidently dependant on the **Y** alkyne substituent. This indicates that chemical modifications on the pyridine (**Y**) are generally more electronically impactful than the amine modifications (**M**, affecting the triazole). Information about the excited state identity and lifetime can be inferred from the shape of the emission spectra.[30] The typical excitation and decay cycle of cyclometallated iridium(III) complexes involves excitation from the ground state to a singlet metal/ligand-ligand charge transfer excited state (MLLCT, d$\pi \rightarrow \pi^*$ transition), followed by intersystem crossing to a triplet ^{3}MLLCT excited state. The decay of this pure excited state is often rapid and is a single peak with a roughly gaussian distribution, such as observed in **Y2** and **Y4** complexes (Figure **6A**). Mixing of the ^{3}MLLCT state with a ligand-centred triplet state, ^{3}LC, can also occur, giving a longer-lived excited state. This is characterized by a peak with a significant shoulder (**Y1** and **Y3**, Figure **6A**). The longevity of the excited state can have significant impacts on the photophysical properties of molecules, including on the generation of through reactive oxygen species (ROS).

To ascertain whether ROS was generated by the **IrCN** library, irradiation at 405 nm with ROS scavengers (ABDA (anthracenediyl-bis(methylene) dimalonic acid) and RNO/histidine (*p*-nitrosodimethylaniline)) was undertaken. ABDA was observed to degrade in the DMSO:PBS media, a known effect upon irradiation below 450 nm.[37] Significantly less ROS was detected for all compounds compared to the $Ru(bpy)_3^{2+}$ (bpy = 2,2'-bipyridyl) control using the RNO/histidine assay.[38] This suggests that ROS generation is occurring at a low rate.

Catalysis

Catalytic testing for the **IrCN** library was attempted for the amine radical transfer (ART) reaction described by Speckmeier and Maier,[39] where a commercially available $[Ir(dF(CF_3)ppy)_2(dtbbpy)]PF_6$ photocatalyst enables a nickel-catalysed Suzuki-Miyaura cross-coupling reaction under ambient conditions. Testing with the commercial photocatalyst gave a conversion to product of 47%, but under the same conditions, no product was detected for any of the **IrCN** library by LC-MS. Even after 18 h of

irradiation, no conversion >2% (See SI, Figure S3-4) was achieved. Coupled with the ROS assay results, it would appear that this library is not particularly photo-active under the tested conditions.

Following combinatorial work on ruthenium arene Schiff-base complexes by Weng *et al.*, we tested the **RuCy** libraries for transfer hydrogenation (TH) catalysis using the Coumarin-N_3 assay developed by the same group.[34] As Coumarin-N_3 is hydrogenated to the amine, it becomes fluorescent, so the formation of the product can be monitored over time. The rationale behind this reaction is to take advantage of high formate concentrations in *E. coli* to hydrogenate azide pro-drugs in bacteria.[40] As can be seen in Figure 6, which shows the change in fluorescence intensity from TH catalysed by the **RuCy** libraries, **RuCy(Tz-4-P)** is generally more active than the **RuCy(Tz-1-MP)** library, with 3 compounds (**M11Y2**, **M13Y2**, **M24Y2**) all having a change in intensity >15000 A.U, comparable with active compounds reported by the Ang group.

Overall, we have demonstrated that these metal complex libraries can be rapidly assessed for photophysical and catalytic properties using 96 well plate-based assays under ambient conditions. We envisage that any property-screening assay that is amenable to a well plate format could be adapted to test these and other combinatorial metal complex libraries to identify ideal compounds. We are currently exploring further optimization of metal scaffolds in this area.

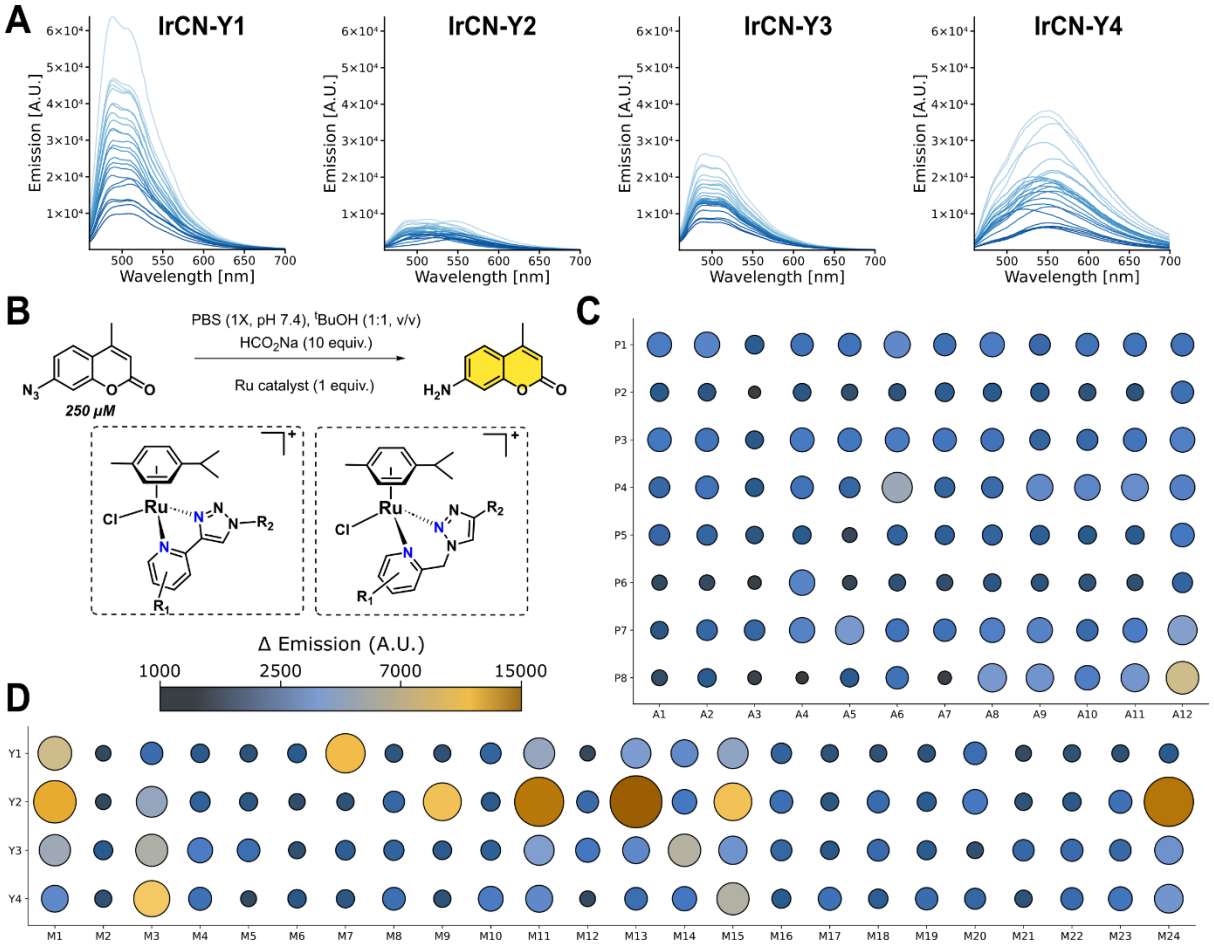

Figure 6: (**A**) Photophysical emission spectra of the **IrCN** library (31.25 μM solutions in DMSO, λ_{ex} = 380 nm); (**B**) scheme for Ru-catalysed transfer hydrogenation of Coumarin-N_3 using the **RuCy** libraries. Heatmaps show the change in fluorescence over 24 h for the reactions (λ_{ex} = 350 nm, λ_{em} = 455 nm), with large dark brown circles showing intensity change >15000 A.U.; (**C**) **RuCy(Tz-1-MP)** library; (**D**) **RuCy(Tz-4-P)** library.

Biological Testing

With the main focus of our group being the exploration of transition metal complexes as antimicrobial agents, we advanced all the prepared libraries to an initial biological assessment. In a primary screening, all crude reaction mixtures were evaluated against two bacterial strains, one Gram-positive (*Staphylococcus aureus*) and one Gram-negative (*Escherichia coli*). As hit-rates against Gram-negative strains are generally much lower due to the complexity of the additional outer-membrane,[41] we decided to evaluate compounds against *E. coli* at 50 μM whereas we tested compounds against *S. aureus* at 12.5 μM and 50 μM to be able to better differentiate the level of activity. Metal-based compounds have a reputation of being generally toxic, although recent reports have questioned this assumption at least in the realm of *in vitro* assays.[8] We therefore tested compounds against human embryonic kidney cells (HEK293T) at 50 μM. Amongst the 192 **Tz-4-P** and **Tz-1-MP** ligands, only one reduced the average viability of HEK293T cells below 50% (**M12Y3**, 45 ± 7% cell viability), showing that the ligands on their own are generally non-toxic (Figure **7A-B**). None of the ligands showed any significant activity against *E. coli*, and only four showed growth inhibition against *S. aureus*: **M7Y1** (50 μM), **M16Y2** (12.5 μM), **M16Y3** (12.5 μM), and **M23Y3** (50 μM). As **M16** contains the broad-spectrum antibiotic ampicillin and the reactions to form those compounds had relatively lower conversion, the observation of some antibacterial activity is unsurprising. We conducted dose-dependent testing of these crudes against *S. aureus* to determine minimum inhibitory concentrations (MIC) of the putative ligands and found them to be 50 μM for **M7Y1** and **M23Y3**, while lower MICs of 12.5 μM and 3.13 μM were observed for the ampicillin containing triazole compounds. Preliminary testing on the metal scaffolds ($[Ir(ppy)_2Cl]_2$, $[Ru(p\text{-cymene})Cl_2]_2$, $Re(CO)_5Cl$, $Mn(CO)_5Br$) showed that only $[Ir(ppy)_2Cl]_2$ had an MIC of 50 μM against *S. aureus*., with the rest having a value >50 μM. Overall, almost all the novel ligands showed no significant antibacterial or cytotoxic properties, and alongside the lack of activity of the metal scaffolds, this allows us to assign any biological effects observed on the metal complex crudes to the putative metal complex with high confidence.

All but one of the **IrCN** complexes showed significant antibacterial activity against *S. aureus* (Figure **7C**). However, none showed any appreciable effect on the growth of *E. coli*. This finding aligns with the general difficulty across the field of (metallo)antibiotic drug discovery to find compounds able to effectively penetrate the double-membrane and evade the efflux pumps of these pathogens.[42,43] Dose-dependent screening of the **IrCN** libraries against *S. aureus* revealed high antibacterial activity. The lowest MIC measured was 0.39 μM for two compounds which is comparable to the standard-of-care antibiotic vancomycin (MIC = 0.42 μM), which was used as a control. Overall, 59 out of 96 compounds displayed an MIC < 5 μM.

A crucial parameter of any antibiotic is its selectivity for bacterial cells over healthy human cells, often denoted by the Therapeutic Index (TI). Unfortunately, most of the **IrCN** also significantly reduced human cell viability at 50 μM. However, given the very high level of antibacterial activity and the observation that the inhibition of a significant portion of the compounds was in the 25–50% range we identified a few compounds with a potentially viable therapeutic index of >10.

The **$Re(CO)_3$** compounds also showed high levels of antibacterial activity in *S. aureus*, with 61 compounds completely inhibiting bacterial growth at 50 μM or lower (Figure **7D**). The MICs were generally higher than for the **IrCN** library, but the compounds were consistently less toxic. Most caused less than 50% growth inhibition in the HEK293T cells, while still having MICs as low as 0.78 μM.

In a comparison of the **$Re(CO)_3$** and **IrCN** libraries, there is a clear mirroring of activity for individual ligands. Generally, if a **$Re(CO)_3$** complex with a given ligand is active, then the corresponding **IrCN** will be equally or more active. This is noteworthy as the ligands themselves are demonstrably not active and the two metal scaffolds are clearly distinct. We speculate that the arrangement of the ligand in an octahedral geometry and the occupation of the coordinating nitrogen atoms with the metal scaffold may be the cause for this.

For the **$Re(CO)_3$** library there is a correlation between its activity and conversion efficiency. The same was not observed for the **IrCN** library. In terms of specific trends, **Y2** and **Y4**-derived ligands are much less active for **$Re(CO)_3$** than **IrCN**, which can be ascribed to lower conversion efficiency in the former. **Y1** and **Y3**-derived ligands are the most active for **$Re(CO)_3$**, with active compounds having similar

activity in both metal libraries. Indeed, **M17–22** for **Y3** show almost identical activity for both **Re(CO)$_3$** and **IrCN**, which suggests that the identity of the metal scaffold is not necessarily important for activity. **M5** (enantiopure *(S)*-1-phenyl-ethylamine)-derived ligands are the overall most active for **Re(CO)$_3$**, and are similarly highly active for **IrCN**, while there was no or very low activity for: **M2** (pendant amide, despite high conversions), **M11** (phenyl-ester, which showed good activity for **IrCN** despite low conversions), **M15** (β-lactam, poor conversions), and **M23** (biaryl, also poor conversions).

By contrast, the **Mn(CO)$_3$** compounds generally showed lower to no significant antibacterial properties than its congener library (Figure **7E**). Only 21 compounds showed any antibacterial activity against *S. aureus* and only 4 had an MIC <10 μM. Nevertheless the overall hit-rate of 21% is comparable to the hit-rate we previously observed in **Mn(CO)$_3$** Schiff-base libraries of 15.3%.[27] The hit-rate is also still much higher compared to what is generally found in purely organic molecule screening campaigns of 0.87%.[43] At the same time this compound class similar rates of cytotoxicity to rhenium, with half of all compounds causing cellular growth inhibition of less than 50% at 50 μM, and a handful causing greater than 75% growth inhibition.

Lastly, the **RuCy** libraries with both **Tz-4-P** and **Tz-1-MP** ligands (Figure **7F-G**) showed the lowest level of antibacterial properties. Only a few of the **RuTz-4-P** compounds inhibited growth against *S. aureus* at 12.5 μM. This is in slight contrast to previous work on ruthenium cymene Schiff-base compounds which have shown high hit-rates and significant antibacterial activity.[26,34,44,45]

In summary we have efficiently evaluated 192 ligands and 480 metal complexes for their antibacterial and cytotoxic properties (an additional 768 **IrCp** compounds are currently undergoing evaluation in ongoing work). This methodology allows us to rapidly narrow our focus on potentially interesting compounds with a desirable therapeutic index, and the combination of single-dose response and full MIC assays on crude reaction mixtures provides key insights into activity trends across metal libraries.

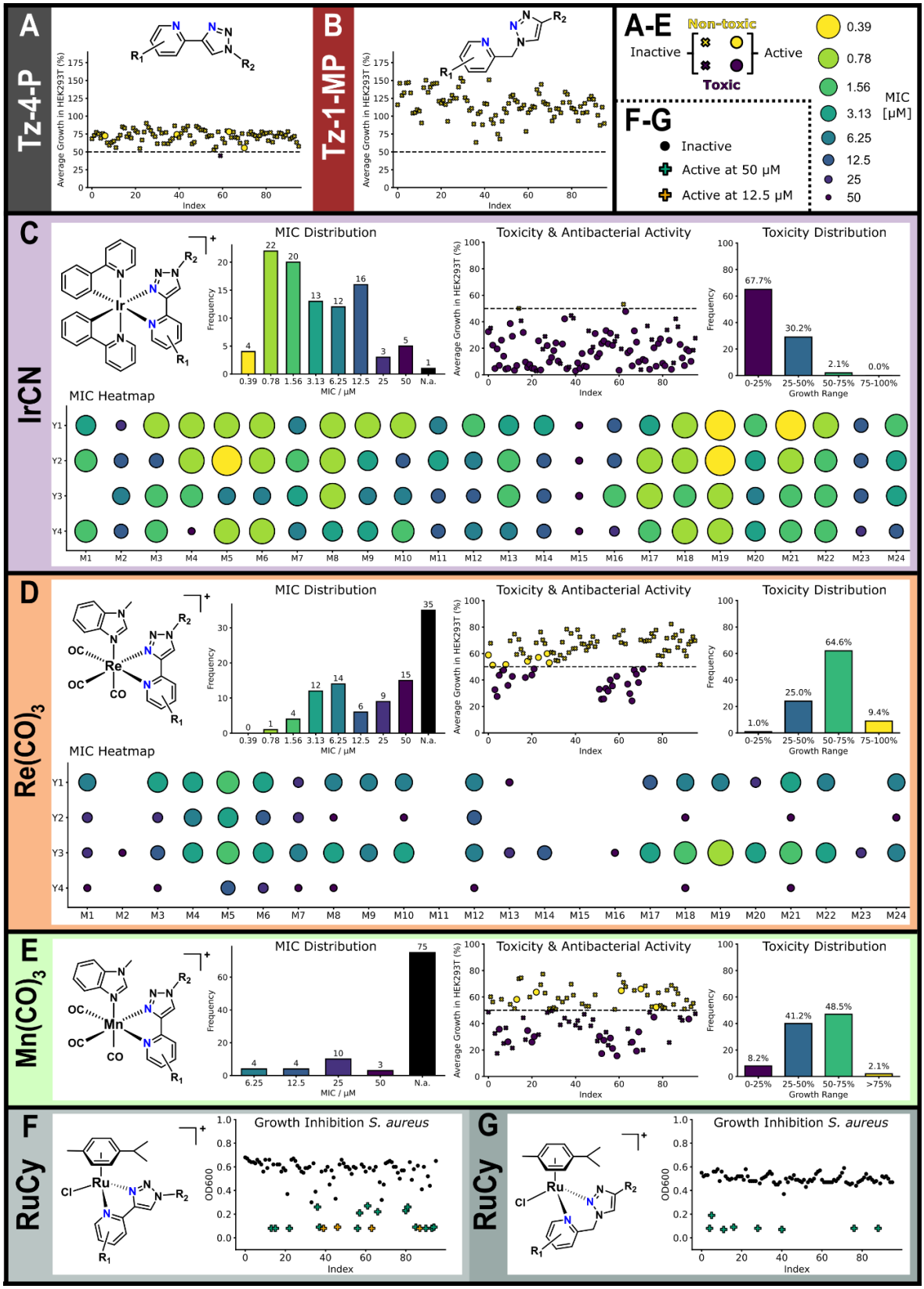

Figure 7: Summary of the biological testing data on the crude ligands and metal complexes prepared in this work. For **A-E**, average % growth of HEK293T cells refers to the toxicity of the compounds at 50 μM (single dose, 2 biological and 2 statistical repeats). Any compounds under 50% (dashed line) are labelled as "toxic". the circles on these graphs refer to whether the compounds had an MIC of ≤ 6.25 μM against *S. aureus*. The MIC heatmaps show at what concentration the compounds fully inhibit growth of *S. aureus* (2 biological and 2 statistical repeats). For **F-G**, only single dose response bacterial data was collected due to low activity, with OD600 (optical density at 600 nm) referring to the concentration of bacteria present after incubation (a low value is classed as "active").

Hit Re-Synthesis and Characterisation

Based on the MIC and single dose response toxicity data of the crude reaction mixtures, 6 complexes were chosen for re-synthesis, full characterisation and re-testing (2x **$Re(CO)_3$**, 2x **IrCN** and 2x **$Mn(CO)_3$**). The criteria for choosing these was based primarily on antimicrobial activity, with the most active complexes identified (nothing with an MIC higher than 6.25 μM was considered). Of these, the least toxic compounds were selected. For the **IrCN** library, as almost all compounds caused less than 50% cell viability, the least toxic compounds with MIC of 1.56 μM were chosen. The **$Re(CO)_3$** appeared to provide a good balance of active compounds with low apparent toxicity, so again the most active and least toxic compounds were chosen. For the **$Mn(CO)_3$** library, only four compounds had an MIC of 6.25 μM, so the purest compounds by LC-MS were selected.

The synthesis of all compounds was achieved by first making the ligands using the scaled-up procedure for generating ligand libraries, changing the solvent from DMSO to DMF to enable a more feasible workup and purification. The ligands were then reacted with the metal in high-yielding reactions. After purification by flash column chromatography, the pure compounds were fully characterized. Single crystals of **$Re(CO)_3$(M1Y1)** were obtained (DCM/hexane slow vapour diffusion), and the X-ray diffraction structure (Figure 8) clearly shows the bidentate binding mode of the **M1Y1** ligand.

Stability assays on the pure compounds were undertaken, with biologically relevant solvents and mixtures tested (DMSO, H_2O, 1X PBS and a combination of DMSO with H_2O and 1X PBS). The stability was ascertained by measurement of UV absorbance (320 nm) at 37 °C over 21 h. All compounds demonstrated good overall stability with less than 10% difference in the spectra over this period, however the **$Mn(CO)_3$** complexes exhibited significant changes in their overall UV-Vis spectra in H_2O and 1X PBS over 2–8 h. This could be due to anion exchange (in the case of PBS), or water competitively binding with the complex in the axial position. However this did not seem to be detrimental to the antibacterial activity of these compounds (*vide infra*).

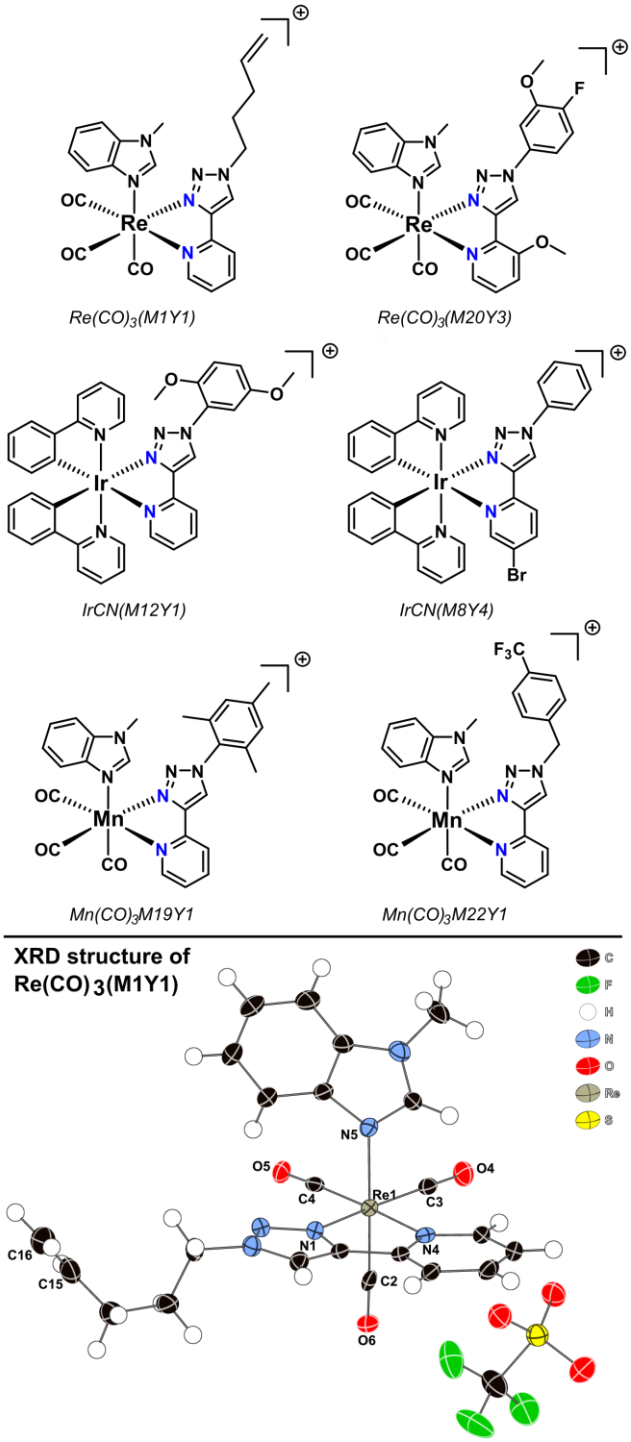

Figure 8: (Top) Chemical structures of lead complexes for re-synthesis and biological testing (MIC and toxicity); (bottom) single crystal X-ray diffraction structure of **$Re(CO)_3$(M1Y1)** (thermal ellipsoids set at 50% probability and hydrogens represented as spheroids). Selected interatomic lengths /Å: Re1-N5 = 2.190(2); Re1-N4 = 2.201(2); Re1-N1 = 2.156(2); Re1-C2 = 1.930(3); Re1-C3 = 1.922(3); Re1-C4 – 1.916(3); C15-C16 = 1.310(5). Selected interatomic angles /°: N1-Re1-N4 = 74.94(8); N1-Re1-N5 = 82.32(8); N4-Re1-N5 = 85.70(8); C3-Re1-C4 = 89.95(11); N1-Re1-C4 = 99.22(9).

Hit Validation

Biological studies were undertaken on the purified compounds to confirm activity against bacteria (MIC assays) and ascertain toxicity (CC_{50} measurements against HEK293T cells). Regarding the bacterial assays, there was almost no activity against *E. coli* at the measured concentrations, with the exception of **$Re(CO)_3$(M1Y1)** and **$Mn(CO)_3$(M22Y1)** (MIC = 100 μM, Table 1). However, perturbation of the outer

membrane by polymyxin B nonapeptide (PMBN) resulted in significant activity against *E. coli* for all compounds.[46] PMBN has no inherent antibacterial activity, but damages and weakens the outer membrane of Gram-negative bacteria by interacting with the anionic lipopolysaccharide molecules. This permeabilizes the membrane to antibiotics, suggesting that uptake into Gram-negative bacteria is the issue for these compounds and they are not necessarily Gram-positive specific.[47]

For the Gram-positive strains, high activity was observed in almost all cases. A comparison of activity between the crude reaction mixtures and re-synthesized compounds against *S. aureus* gives an increase in activity in all cases, with very low MICs (5 compounds active in the nanomolar range similar to the vancomycin control MIC = 0.42 µM, Table 1). This confirms that in all cases it is the putative metal complex in the crudes that is responsible for the observed activity, hence validating our methodology of pre-screening large crude libraries (Table 1). It should be noted that in several cases (**$Re(CO)_3$(M1Y1), IrCN(M12Y1), $Mn(CO)_3$(M19Y1)**) there were larger increases (>16x, >4x, and >8x more active respectively) in antibacterial activity than expected from the increase in purity due to re-synthesis (crude purity by LC-MS of 43%, 72%, 41% respectively). This suggests that our methodology in fact underestimates the activity of the complexes in the synthesized libraries.

The other tested Gram-positive strains showed generally good activity, with slightly higher MICs against *Enterococcus faecalis* in most cases. The exception was the manganese complexes, which were significantly less active. *Enterococcus faecium* showed very low growth in the Mueller-Hinton (MH) growth medium that was typically used, so Tryptic Soy Broth (TSB) growth medium was used instead. This gave measurable MICs, but a comparison with *E. faecalis* (which was tested in both MH and TSB) indicates that TSB results in a significant rise in MIC values. As such, although the MICs for *E. faecium* are higher than *S. aureus*, there is still good activity in most cases (Table 1). Generally, **$Re(CO)_3$(M20Y3)** and **IrCN(M12Y1)** show exceptional activity across the tested Gram-positive (and sensitized Gram-negative) bacterial strains, with often nanomolar MICs. The fact that the compounds showed very low MICs against *E. coli* upon permeabilization suggests that further structural optimisation targeted at improving Gram-negative bacterial uptake could result in pan-active metalloantibiotics. As the antibacterial activity of the pure compounds increased compared to the crudes, the same trend was also observed for their cytotoxicity. Indeed, most of the compounds displayed CC_{50} in the range of 10 µM. However, due to their high level of antibacterial activity all compounds except **$Mn(CO)_3$(M22Y1)** still displayed a favorable therapeutic index >10. The best ratio of antibacterial activity and toxicity was determined for **IrCN(M8Y4)** showcasing a therapeutic index between 49–99. Overall, these values are comparable and in several cases superior to that of other recently reported metal-based antibiotics.[13,20,27]

Table 1: Minimum Inhibitory Concentration (MIC) and toxicity data for the re-synthesized compounds against a selection of Gram-positive and Gram-negative strains. Antibacterial activity is displayed as MIC [µM]. A "-" indicates no activity up to 100 µM; PMBN – polymyxin B nonapeptide sensitizer (10 µg / mL); CC50 – HEK293T cells, the error recorded is the standard deviation; TI – therapeutic index, determined by dividing the lowest value between CC_{50} and with the lowest MIC value for each compound against *S. aureus*; VAN – vancomycin. MIC determined with n = 3 across two biological replicates; [a)]TSB growth medium used.

	MIC [µM] *vs.* bacteria						Toxicity [µM]		
	S. aureus		*E. faecium*[a)]	*E. faecalis*	*E. coli*	*E. coli* + PMBN	Crude toxicity (%viability, 50 µM)	CC_{50}	TI
	Crude	Pure							
$Re(CO)_3$(M1Y1)	6.25 – 12.5	0.39	12.5	1.56 – 3.13	100	6.25 - 25	59 ± 8	12.4 ± 1.2	32
$Re(CO)_3$(M20Y3)	3.13 – 6.25	0.39 – 0.78	3.13	0.78 – 1.56	-	3.13 – 6.25	47 ± 8	8.2 ± 0.7	11 – 21
IrCN(M12Y1)	1.56 – 3.13	0.20 – 0.39	3.13	1.56	-	0.78 – 1.56	29 ± 3	7.3 ± 1.2	19 – 37
IrCN(M8Y4)	1.56 – 3.13	0.39 – 0.78	6.25	1.56 – 3.13	-	3.13 – 6.25	27 ± 6	38.5 ± 5.5	49 – 99
$Mn(CO)_3$(M19Y1)	6.25	0.39 – 0.78	12.5	3.13 – 6.25	-	3.13 – 6.25	35 ± 12	11.9 ± 1.1	15 – 31
$Mn(CO)_3$(M22Y1)	6.25	3.13 – 6.25	25	12.5 – 25	100	12.5 – 25	30 ± 18	12.9 ± 1.2	2 – 4
Vancomycin [µg / mL]	0.625	0.625	0.625	0.313					
Polymyxin B [µg / mL]					0.313	0.313			

From a methodology perspective, the single dose toxicity assay was used as a guide to select the most active and least toxic compounds for re-synthesis. It is clear from the CC_{50} data that although the single dose assay mirrors the true toxicity, it can underestimate the cytotoxicity of compounds. For the **IrCN** compounds, it was expected that they would have significant toxicity based on recent work, and the single dose assay did indeed indicate that.[19] More surprising is the **Re(CO)$_3$** data, which was significantly more toxic than expected from the preliminary assay. As such, the high throughput assay does successfully indicate toxicity, but more stringent conditions on selecting active and non-toxic compounds will be used in future work, such as increasing the toxicity threshold above 50% cell viability. It should be noted that cell-based assays can only provide so much information and hit compounds will have to undergo more stringent testing before a conclusion can be made about their safety.

Summary and Conclusions

In summary, we have presented a new combinatorial methodology to generate large libraries of pyridyl-triazole bidentate ligands formed by CuAAc Click reactions. These libraries have been demonstrated to coordinate efficiently to a number of metal scaffolds, generating 672 novel, well-characterized complexes under mild conditions. Although not the main focus of this work, we have showcased some applications of our metal libraries for (photo)catalytic and photophysical studies and screening. We have successfully screened all compounds for antimicrobial activity and toxicity in a high-throughput manner, and, using the available data, have re-synthesized several highly active metalloantibiotics, with MICs as low as 200 nM against *S. aureus*. We have also demonstrated that the single-dose antibacterial and toxicity assays are a reliable indicator of the properties of the pure compounds from crude reaction mixtures, even for low-yielding reactions. However, care must be taken when it comes to single-dose toxicity assays as they tended to indicate that compounds were less toxic than they turned out to be upon re-synthesis.

Although promising activity against Gram-positive bacteria has been reported here for a number of different metal complexes, activity against Gram-negative strains has been lacking. Improved activity in the presence of the PMBN sensitizer suggests that the low original activity is in part due to poor uptake of the synthesized metal complexes. However, thanks to the combinatorial and versatile ligand architecture there is now scope to significantly vary the ligands to explore and include motifs to improve uptake into bacteria.[48,49]

The potential scope of this ligand chemistry is somewhat limited by the availability of 2-alkyne pyridines (for the **Tz-4-P** library). However, this limitation is more than made up for by the capacity to use practically any primary amine to generate bidentate ligands, and hence a staggering number of novel metal complexes are now obtainable. Additionally, as the ligand architecture remains constant but is highly variable, this methodology lends itself well to potential machine learning applications to enable the discovery of ever more potent antibiotics.[26] In terms of other biological applications, assays for any disease-based screening would in principle be possible on these libraries or derivatives of them.

Work in our group is currently ongoing with derivatives of **IrCN** and **IrCp*** libraries to further explore photophysical properties, photodynamic therapy, and catalytic applications. We believe there is much scope to expand the types of chemistry that are amenable to the combinatorial generation of novel ligand structures. Additionally, we have only scratched the surface of the periodic table in terms of explored metal scaffolds. While each metal may require slightly different conditions and not all of them will be amenable to this type of chemistry, we believe that the field of combinatorial metal complex synthesis is only just at its beginning.

Declaration

The authors declare that all data supporting the current findings of this study are available in the main manuscript or in the Supplementary information. The single crystal datum (including a cif. file and a structural figure) of **$Re(CO)_3$(M1Y1)** was uploaded to Cambridge Structural Database, obtaining corresponding CCDC number 2455425. The data related to the figures and other findings of this study are available from the corresponding author upon request.

Competing interests

The authors declare no competing interests.

Contribution

A.F devised and directed the project. A.W and C.O performed the toxicity studies and processed the data. R.G. was the crystallographer for the XRD structure. D.R.H performed all other experimental work and processing.

Acknowledgements

The authors wish to thank the University of York for supporting the project. Funding from the Swiss National Science Foundation in the form of an Ambizione (PZ00P2_202016) and COST-Project Grant (IZCOZ0_220299) is gratefully acknowledged. Thanks also to Prof. Anne-Kathrin Duhme-Klair and Niall Donaldson for their support in setting up the lab, Prof. Ronan McCarthy (Brunel) for providing the bacterial strains, CHyME at the University of York for biolab access and Dr. Lianne Willems for the HEK293T cells. Dr Ed Bergstrom and the COEMS (York) for the use of LC-MS equipment and Karl Heaton and Dr. Matthew Davy for mass spectrometry and NMR support respectively.

References

1 E. Haldón, M. C. Nicasio and P. J. Pérez, *Org. Biomol. Chem.*, 2015, **13**, 9528–9550.
2 M. C. Joseph, A. J. Swarts and S. F. Mapolie, *Coord. Chem. Rev*, 2023, **493**, 215317.
3 P. A. Scattergood and P. I. P. Elliott, *Dalton Trans.*, 2017, **46**, 16343–16356.
4 J. D. Crowley and D. A. McMorran, in *Click Triazoles*, ed. J. Košmrlj, Springer, Berlin, Heidelberg, 2012, pp. 31–83.
5 W. K. C. Lo, G. S. Huff, J. R. Cubanski, A. D. W. Kennedy, C. J. McAdam, D. A. McMorran, K. C. Gordon and J. D. Crowley, *Inorg. Chem.*, 2015, **54**, 1572–1587.
6 P. M. Guha, H. Phan, J. S. Kinyon, W. S. Brotherton, K. Sreenath, J. T. Simmons, Z. Wang, R. J. Clark, N. S. Dalal, M. Shatruk and L. Zhu, *Inorg. Chem.*, 2012, **51**, 3465–3477.
7 W. Stroek and M. Albrecht, *Chem. Soc. Rev.*, 2024, **53**, 6322–6344.
8 A. Frei, A. D. Verderosa, A. G. Elliott, J. Zuegg and M. A. T. Blaskovich, *Nat. Rev. Chem.*, 2023, **7**, 202–224.
9 WHO, Antimicrobial resistance, https://www.who.int/news-room/fact-sheets/detail/antimicrobial-resistance, (accessed 29 May 2025).
10 C. J. L. Murray, K. S. Ikuta, F. Sharara, L. Swetschinski, G. R. Aguilar, A. Gray, C. Han, C. Bisignano, P. Rao, E. Wool, S. C. Johnson, A. J. Browne, M. G. Chipeta, F. Fell, S. Hackett, G. Haines-Woodhouse, B. H. K. Hamadani, E. A. P. Kumaran, B. McManigal, S. Achalapong, R. Agarwal, S. Akech, S. Albertson, J. Amuasi, J. Andrews, A. Aravkin, E. Ashley, F.-X. Babin, F. Bailey, S. Baker, B. Basnyat, A. Bekker, R. Bender, J. A. Berkley, A. Bethou, J. Bielicki, S. Boonkasidecha, J. Bukosia, C. Carvalheiro, C. Castañeda-Orjuela, V. Chansamouth, S. Chaurasia, S. Chiurchiù, F. Chowdhury, R. C. Donatien, A. J. Cook, B. Cooper, T. R. Cressey, E. Criollo-Mora, M. Cunningham, S. Darboe, N. P. J. Day, M. D. Luca, K. Dokova, A. Dramowski, S. J. Dunachie, T. D. Bich, T. Eckmanns, D. Eibach, A. Emami, N. Feasey, N. Fisher-Pearson, K. Forrest, C. Garcia, D. Garrett, P. Gastmeier, A. Z. Giref, R. C. Greer, V. Gupta, S. Haller, A. Haselbeck, S. I. Hay, M. Holm, S. Hopkins, Y. Hsia, K. C. Iregbu, J. Jacobs, D. Jarovsky, F. Javanmardi, A. W. J. Jenney, M. Khorana, S. Khusuwan, N. Kissoon, E. Kobeissi, T. Kostyanev, F. Krapp, R. Krumkamp, A. Kumar, H. H. Kyu, C. Lim, K. Lim, D. Limmathurotsakul, M. J. Loftus, M. Lunn, J. Ma, A. Manoharan, F. Marks, J. May, M. Mayxay, N. Mturi, T. Munera-Huertas, P. Musicha, L. A. Musila, M. M. Mussi-Pinhata, R. N. Naidu, T. Nakamura, R. Nanavati, S. Nangia, P. Newton, C. Ngoun, A. Novotney, D. Nwakanma, C. W. Obiero, T. J. Ochoa,

A. Olivas-Martinez, P. Olliaro, E. Ooko, E. Ortiz-Brizuela, P. Ounchanum, G. D. Pak, J. L. Paredes, A. Y. Peleg, C. Perrone, T. Phe, K. Phommasone, N. Plakkal, A. Ponce-de-Leon, M. Raad, T. Ramdin, S. Rattanavong, A. Riddell, T. Roberts, J. V. Robotham, A. Roca, V. D. Rosenthal, K. E. Rudd, N. Russell, H. S. Sader, W. Saengchan, J. Schnall, J. A. G. Scott, S. Seekaew, M. Sharland, M. Shivamallappa, J. Sifuentes-Osornio, A. J. Simpson, N. Steenkeste, A. J. Stewardson, T. Stoeva, N. Tasak, A. Thaiprakong, G. Thwaites, C. Tigoi, C. Turner, P. Turner, H. R. van Doorn, S. Velaphi, A. Vongpradith, M. Vongsouvath, H. Vu, T. Walsh, J. L. Walson, S. Waner, T. Wangrangsimakul, P. Wannapinij, T. Wozniak, T. E. M. W. Y. Sharma, K. C. Yu, P. Zheng, B. Sartorius, A. D. Lopez, A. Stergachis, C. Moore, C. Dolecek and M. Naghavi, *The Lancet*, 2022, **399**, 629–655.
11 M. S. Butler, I. R. Henderson, R. J. Capon and M. A. T. Blaskovich, *J. Antibiot.*, 2023, **76**, 431–473.
12 R. G. Miller, M. Vázquez-Hernández, P. Prochnow, J. E. Bandow and N. Metzler-Nolte, *Inorg. Chem.*, 2019, **58**, 9404–9413.
13 S. V. Kumar, S. Ø. Scottwell, E. Waugh, C. J. McAdam, L. R. Hanton, H. J. L. Brooks and J. D. Crowley, *Inorg. Chem.*, 2016, **55**, 9767–9777.
14 K. L. Smitten, P. A. Scattergood, C. Kiker, J. A. Thomas and P. I. P. Elliott, *Chem. Sci.*, 2020, **11**, 8928–8935.
15 S. V. Kumar, W. K. C. Lo, H. J. L. Brooks, L. R. Hanton and J. D. Crowley, *Aust. J. Chem.*, 2015, **69**, 489–498.
16 S. Friães, C. Trigueiros, C. S. B. Gomes, A. R. Fernandes, O. A. Lenis-Rojas, M. Martins and B. Royo, *Molecules*, 2023, **28**, 7453.
17 I. Kacsir, A. Sipos, G. Ujlaki, P. Buglyó, L. Somsák, P. Bai and É. Bokor, *Int. J. Mol. Sci.*, 2021, **22**, 10454.
18 G. J. Barbante, E. H. Doeven, E. Kerr, T. U. Connell, P. S. Donnelly, J. M. White, T. Lópes, S. Laird, D. J. D. Wilson, P. J. Barnard, C. F. Hogan and P. S. Francis, *Chem. Eur. J.*, 2014, **20**, 3322–3332.
19 T. Kench, A. Rahardjo, G. G. Terrones, A. Bellamkonda, T. E. Maher, M. Storch, H. J. Kulik and R. Vilar, *Angew. Chem. Int. Ed.*, 2024, **63**, e202401808.
20 T. Kench, N. Sultana Chowdhury, K. M. Rahman and R. Vilar, *Inorg. Chem.*, 2025, **64**, 5113–5121.
21 D. Hernández-Romero, S. Rosete-Luna, E. Méndez-Bolaina, E. de la C. Herrera-Cogco, L. P. Amador-Gómez, A. Soto-Contreras, J. M. Rivera-Villanueva and R. Colorado-Peralta, *Reactions*, 2024, **5**, 947–983.
22 A. Kafle and S. T. Handy, *Tetrahedron*, 2017, **73**, 7024–7029.
23 S. Bräse, C. Gil, K. Knepper and V. Zimmermann, *Angew. Chem. Int. Ed.*, 2005, **44**, 5188–5240.
24 G. Meng, T. Guo, T. Ma, J. Zhang, Y. Shen, K. B. Sharpless and J. Dong, *Nature*, 2019, **574**, 86–89.
25 A. Welsh, D. Husbands and A. Frei, *Angew. Chem. Int. Ed.*, 2025, **64**, e202420204.
26 M. Orsi, B. Shing Loh, C. Weng, W. H. Ang and A. Frei, *Angew. Chem. Int. Ed.*, 2024, **63**, e202317901.
27 M. Scaccaglia, M. P. Birbaumer, S. Pinelli, G. Pelosi and A. Frei, *Chem. Sci.*, 2024, **15**, 3907–3919.
28 N. Hulstaert, J. Shofstahl, T. Sachsenberg, M. Walzer, H. Barsnes, L. Martens and Y. Perez-Riverol, *J. Proteome. Res.*, 2020, **19**, 537–542.
29 M. A. Sierra, L. Casarrubios and M. C. de la Torre, *Chem. Eur. J.*, 2019, **25**, 7232–7242.
30 S. DiLuzio, V. Mdluli, T. U. Connell, J. Lewis, V. VanBenschoten and S. Bernhard, *J. Am. Chem. Soc.*, 2021, **143**, 1179–1194.
31 L. Cattalini, A. Cassol, G. Marangoni, G. Rizzardi and E. Rotondo, *Inorganica Chim. Acta*, 1969, **3**, 681–684.
32 D. Urankar, A. Pevec, I. Turel and J. Košmrlj, *Cryst. Growth Des*, 2010, **10**, 4920–4927.
33 A. Maisonial, P. Serafin, M. Traïkia, E. Debiton, V. Théry, D. J. Aitken, P. Lemoine, B. Viossat and A. Gautier, *Eur. J. Inorg. Chem.*, 2008, **2008**, 298–305.
34 C. Weng, L. Shen and W. H. Ang, *Angew. Chem. Int. Ed.*, 2020, **59**, 9314–9318.
35 T. T. Talele, *J. Med. Chem.*, 2018, **61**, 2166–2210.
36 R. Keese and M. Meyer, *Tetrahedron*, 1993, **49**, 2055–2064.
37 T. Entradas, S. Waldron and M. Volk, *J. Photochem. Photobiol. B*, 2020, **204**, 111787.
38 A. Frei, R. Rubbiani, S. Tubafard, O. Blacque, P. Anstaett, A. Felgenträger, T. Maisch, L. Spiccia and G. Gasser, *J. Med. Chem.*, 2014, **57**, 7280–7292.
39 E. Speckmeier and T. C. Maier, *J. Am. Chem. Soc.*, 2022, **144**, 9997–10005.
40 G. Unden and J. Bongaerts, *Biochim. Biophys. Acta*, 1997, **1320**, 217–234.
41 A. H. Delcour, *Biochim. Biophys. Acta*, 2009, **1794**, 808–816.
42 R. Kumari and I. Saraogi, *ChemPhysChem*, 2025, **26**, e202401057.
43 A. Frei, J. Zuegg, A. G. Elliott, M. Baker, S. Braese, C. Brown, F. Chen, C. G. Dowson, G. Dujardin, N. Jung, A. P. King, A. M. Mansour, M. Massi, J. Moat, H. A. Mohamed, A. K. Renfrew, P. J. Rutledge,

P. J. Sadler, M. H. Todd, C. E. Willans, J. J. Wilson, M. A. Cooper and M. A. T. Blaskovich, *Chem. Sci.*, 2020, **11**, 2627–2639.
44 C. Weng, L. Shen, J. W. Teo, Z. C. Lim, B. S. Loh and W. H. Ang, *JACS Au*, 2021, **1**, 1348–1354.
45 C. Weng, H. Yang, B. S. Loh, M. W. Wong and W. H. Ang, *J. Am. Chem. Soc.*, 2023, **145**, 6453–6461.
46 M. Vaara, *Microbiol. Rev.*, 1992, **56**, 395–411.
47 M. Vaara, *Molecules*, 2019, **24**, 249.
48 H.-K. Ropponen, R. Richter, A. K. H. Hirsch and C.-M. Lehr, *Adv. Drug Deliv. Rev*, 2021, **172**, 339–360.
49 B. Rayner, A. D. Verderosa, V. Ferro and M. A. T. Blaskovich, *RSC Med. Chem.*, 2023, **14**, 800–822.